Vehicle Steering Control with Lateral and Angular Misalignment Estimation Based on Receiver Current in Dynamic Wireless Power Transfer

Ryota Tauchi*, Yusaku Takagi†, Osamu Shimizu†, Hiroshi Fujimoto†
*Graduate School of Engineering, The University of Tokyo, Kashiwa, Japan
Email: tauchi.ryota24@ae.k.u-tokyo.ac.jp
†Graduate School of Frontier Sciences, The University of Tokyo, Kashiwa, Japan
Email: {takagi.yusaku22@ae.k.u-tokyo.ac.jp, shimizu.osamu@edu.k.u-tokyo.ac.jp, fujimoto@k.u-tokyo.ac.jp}

***Abstract*—This paper proposes a receiver-side DC current-based method for vehicle lateral and angular misalignment estimation in dynamic wireless power transfer (DWPT) systems. The proposed method uses a current-map that formulates the relationship between lateral misalignment and DC current on the receiver side. In addition, this paper focuses on angular misalignment estimation. This is accomplished by the derivation of geometric relationships from two or more estimated values of lateral misalignment on each transmitter coil. From the simulation and experiment, the proposed method was confirmed to be effective when angular misalignment of the vehicle body occurs, such as when changing lanes.**

***Index Terms*—electric vehicle, dynamic wireless power transfer, lateral misalignment, angular misalignment**

I. Introduction

In recent years, electric vehicles (EVs) have become increasingly popular worldwide due to their low environmental impact [1]. However, their popularization has been constrained by the limited driving range, the long time required for charging, and the necessity of larger and heavier batteries to achieve greater range, which increases the weight and cost of vehicles. Dynamic wireless power transfer (DWPT) is a key technology to address such weaknesses of EVs [2], [3]. DWPT is a technology that wirelessly supplies electric power to an EV in motion and charges the battery. It uses electromagnetic induction to send power from a transmitter coil embedded in a road to a receiver coil mounted on the vehicle. DWPT can extend the driving range of EVs, shorten their charging time, and reduce their cost by suppressing battery capacity, which can contribute to reducing greenhouse gas emissions [4]. However, misalignment between the transmitter coil and the receiver coil negatively impacts mutual inductance, leading to a reduction in both power transfer efficiency and system performance.

Some studies focus on misalignment estimation in DWPT. For example, methods that utilize magnetic sensors [5]–[7], cameras mounted on EVs [8], [9], or sensor coils on the receiver side or the power transmitter side to estimate lateral misalignment (LM) [10]–[12] have been proposed in conventional research. Other studies have utilized integrated inductors on the receiver side as sensor coils [13] or RFID sensing [14]. However, these methods have the disadvantage of increased implementation costs due to additional sensors and susceptibility to the external environment. Thus, a “sensorless” approach is needed in research about DWPT misalignment estimation.

Some research has been studying a method of estimating misalignment that does not require an external sensor by using electrical information such as DC voltage or current in a DWPT circuit [15]–[17]. For example, a method has been proposed that utilizes receiver side DC current to estimate LM [17]. This study also proposed an active vehicle steering control system considering vehicle dynamics to compensate for LM, which was validated by experiments using an experimental electric vehicle. However, angular misalignment (AM), or vehicle yaw angle, which can occur due to various driving maneuvers such as lane changes, was not considered. This results in a deterioration in estimation accuracy and control performance. Therefore, in this paper, a new AM estimation method based on receiver side DC current is proposed.

This paper is organized as follows. Section II discusses how LM is estimated based on receiver side DC current. Section III presents how AM can be estimated in DWPT systems. In section IV, simulation results are shown to illustrate how much accuracy in AM estimation is required. Section V describes experiments using an experimental EV. In section VI, the main paper achievements are summarized, and a plan for future work is outlined.

II. DC current-map for LM estimation

This section describes the method for estimating LM in DWPT systems based on DC current on the receiver side, without relying on external sensors. The circuit model of DWPT used in this study is shown in Fig. 1. R, L, C, V, and I represent the parasitic resistance, self-inductance of the coil, capacitance, voltage, and current. Additionally, L_{m} represents the mutual inductance between the transmitter and receiver coils. Assuming that complete resonance is achieved on the transmitter and receiver sides, in other words, the inverter

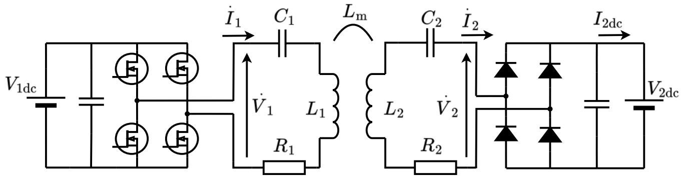

Fig. 1: System Configuration of DWPT.

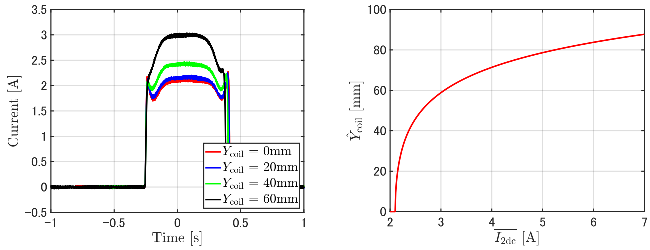

(a) (b)

Fig. 2: Current-map derivation. (a) Current waveform for different $Y_{\rm coil}$. (b) Current-map for LM estimation.

operating angular frequency ω can be expressed as:

$$\omega = \frac{1}{\sqrt{L_1 C_1}} = \frac{1}{\sqrt{L_2 C_2}}, \tag{1}$$

then, I_2 and V_2 can be expressed as:

$$I_2 = \frac{\omega L_{\rm m}}{(\omega L_{\rm m})^2 + R_1(R_2 + R_{\rm L})} V_1, \tag{2}$$

$$V_2 = \frac{\omega L_{\rm m} R_{\rm L}}{(\omega L_{\rm m})^2 + R_1(R_2 + R_{\rm L})} V_1, \tag{3}$$

where $R_{\rm L}$ represents load resistance on the receiver side. Eliminating $R_{\rm L}$ from the above equations, I_2 can be expressed as:

$$I_2 = \frac{\omega L_{\rm m} V_1 - R_1 V_2}{(\omega L_{\rm m})^2 + R_1 R_2}. \tag{4}$$

Thus, DC current on the receiver side, $I_{\rm 2dc}$, can be expressed as:

$$I_{\rm 2dc} \simeq \frac{2\sqrt{2}}{\pi} I_2 = \frac{8}{\pi^2} \frac{\omega L_{\rm m} V_{\rm 1dc} - R_1 V_{\rm 2dc}}{\omega^2 {L_{\rm m}}^2 + R_1 R_2}. \tag{5}$$

When misalignment between the transmitter coil and receiver coil occurs, coupling between them becomes lower, resulting in lower $L_{\rm m}$. Therefore, the larger misalignment becomes, the larger $I_{\rm 2dc}$ becomes as shown in Fig. 2(a). $Y_{\rm coil}$, the LM, is defined as the distance between the center line of the transmitter coil and the center of gravity of the receiver coil. In the conventional study [17], this relationship is heuristically formulated as:

$$\hat{Y}_{\rm coil} = \frac{1}{b} \text{arccosh} \left(\frac{\overline{I_{\rm 2dc}} - c}{a} \right), \tag{6}$$

where a, b, and c are fitting parameters. $\overline{I_{\rm 2dc}}$ represents the mean value of $I_{\rm 2dc}$ in a region where coupling change in the longitudinal direction is negligible. The approximate form of this formula is shown in Fig. 2(b). Using this formula, LM can be estimated from electrical information in the DWPT system, DC current, without using external sensors for self-position estimation.

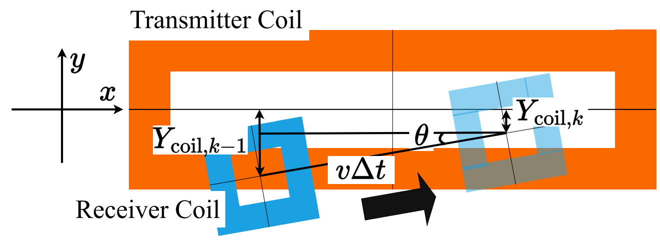

Fig. 3: Angular misalignment estimation.

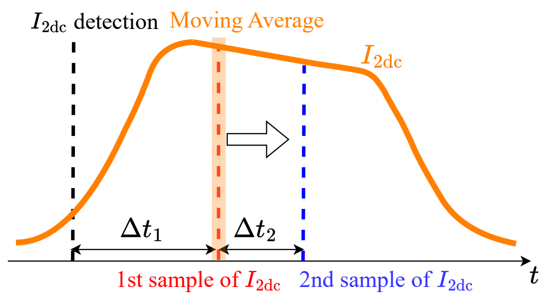

Fig. 4: Two sampling points of $I_{\rm 2dc}$.

III. Angular Misalignment Estimation

In this section, a method to estimate AM based on the DC current-map is proposed. AM can be illustrated as shown in Fig. 3. This image shows a vehicle passing over a transmitter coil. $Y_{{\rm coil},k-1}$, $Y_{{\rm coil},k}$, and θ represent the $k-1$ th and k th sampled LMs and AM. Additionally, v and Δt are the vehicle speed and sampling period. From the geometric relationship between LM and AM in Fig. 3, AM can be expressed as:

$$\hat{\theta} = \sin^{-1} \left(\frac{Y_{{\rm coil},k-1} - Y_{{\rm coil},k}}{v \Delta t} \right). \tag{7}$$

In this equation, careful consideration must be given as to when to sample the LM from the current-map shown in Fig. 2(b). Since the current-map can be utilized only in the region where coupling between transmitter coil and receiver coil is high and coupling change in the longitudinal direction is negligible, an algorithm that samples LM more than once within that region is needed. To achieve this, when to sample DC current and calculate $Y_{\rm coil}$ from Eq. (6) is decided based on the mutual inductance between the transmitter and receiver coils. An illustration of the sampling method is shown in Fig. 4. In this figure, the approximate shape of the $I_{\rm 2dc}$ waveform is shown as the vehicle approaches and passes over the transmitter coil. First, after detecting the rise of $I_{\rm 2dc}$, the first LM estimation using Eq. (6) is conducted after period Δt_1 [s]. Then, after another period Δt_2 [s], the second LM estimation is conducted, and the AM is estimated according to

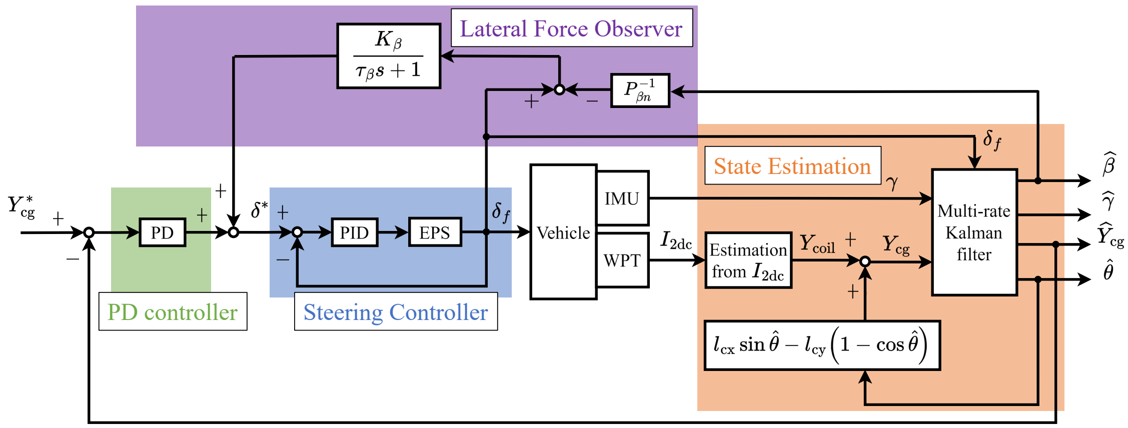

Fig. 5: Block diagram of vehicle steering control system.

Eq. (7). Δt_1 is the time interval from the vehicle detecting I_{2dc} to the region where the coupling is stable, and Δt_2 is the time interval from the first current sampling to the second sampling. Each is determined by measuring the mutual inductance of the transmitter and receiver coil used in the experiment at each position in advance. Δt_1 and Δt_2 can be expressed as:

$$\Delta t_1 = \frac{l_1}{v}, \tag{8}$$

$$\Delta t_2 = \frac{l_2}{v}, \tag{9}$$

where l_1 and l_2 are the distance the vehicle travels from I_{2dc} detection to coupling stabilization and from the first I_{2dc} sampling to the second I_{2dc} sampling, respectively.

IV. Simulation

A. Simulation condition

In this section, simulations were performed to compare the proposed and conventional methods. The simulations compared the conventional method with the case where the initial value of the estimated AM, $\hat{\theta}_0$, is given with an error of $\varepsilon = 1$ [deg] to the true value. Additionally, the initial value of the LM from the vehicle center of gravity, Y_{cg0}, was adjusted so that Y_{coil} at the passage of the first coil was 50 [mm] for all patterns. In this study, automated steering control is utilized to control the vehicle's LM. The block diagram of the control system is shown in Fig. 5. The controller consists of a PD controller and a disturbance observer with feedback of $\hat{Y}_{cg}$. Additionally, the state estimation is conducted by the multi-rate kalman filter proposed in the conventional study [17]. Inputs to the Kalman filter are the vehicle steering angle, LM from the current map, and yaw rate from an inertial measurement unit (IMU). Here, a situation where a vehicle enters the DWPT lane at an angle to the DWPT lane is assumed, as shown in Fig. 6. The first coil is located at $x = 2$ [m]. The state estimation starts when the vehicle passes the first transmitter coil. Specific simulation parameters are listed in TABLE I. $Q_{Y_{cg}}$, Q_θ, $R_{Y_{cg}}$, τ_β, and K_β represent the process noise of Y_{cg} and θ, observed noise of Y_{cg}, time constant of the differentiator, and the gain of the disturbance observer respectively.

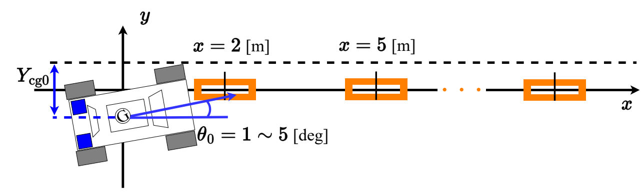

Fig. 6: Situation where a vehicle enters the DWPT lane at an angle.

TABLE I: Simulation Condition.

Parameter	Value	unit
v	1.00	m/s
$Q_{Y_{cg}}$	1.00×10^{-11}	-
Q_θ	1.00×10^{-10}	-
$R_{Y_{cg}}$	1.00×10^{-3}	-
τ_β	5.00×10^{-2}	s
K_β	4.00×10^{-1}	-

B. Vehicle Steering Control Simulation

A comparison of responses when $\theta_0 = 2$ [deg] is shown in Fig. 7. The yellow shaded area indicates the regions where power is transferred from the transmitter coils. In the conventional method ($\hat{\theta}_0 = 0$ [deg]), the estimation accuracy of Y_{cg} is poor, causing oscillation due to the large discrepancy between θ_0 and $\hat{\theta}_0$. Additionally, there are regions where the LM is too large, and the power is not being transferred despite the presence of a transmitter coil. In contrast, when $\hat{\theta}_0 = \theta_0 - \varepsilon$, estimation accuracy improves, and appropriate steering input prevents large LM. Root mean squared error (RMSE) values of Y_{cg} for 0 [mm] of each pattern are shown in Table II. As the AM increases, if $\hat{\theta}_0 = 0$, the initial estimation error is too large to provide an appropriate control input, steering angle, and the system will diverge before it reaches the second and subsequent transmitter coils. From the simulation, if the error ε is within about 1 [deg] of the true value, it is possible to obtain a better response than with conventional methods in steering angle control.

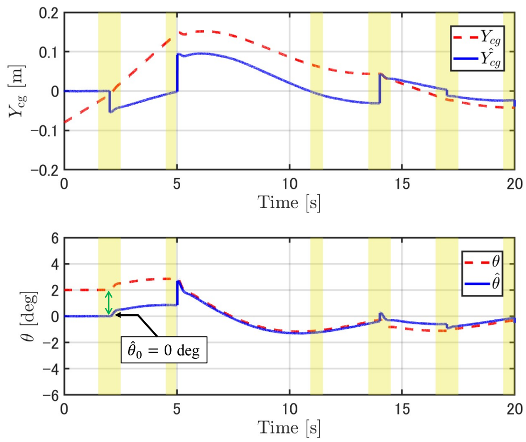

(a) Conventional method ($\theta_0 = 2$ [deg]).

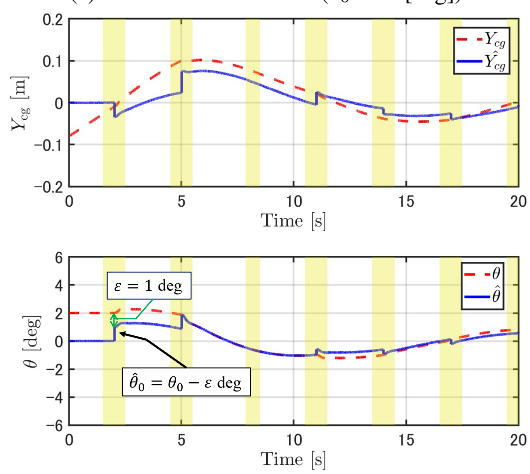

(b) $\hat{\theta}_0 = \theta_0 - \varepsilon$ [deg].

Fig. 7: Simulation results ($\theta_0 = 2$ [deg]).

TABLE II: Y_{cg} RMSE comparison.

	RMSE [m]	
	$\hat{\theta}_0 = \theta_0 - \varepsilon$ [deg]	Conventional method ($\hat{\theta}_0 = 0$ [deg])
$\theta_0 = 2$	0.0546	0.0814
$\theta_0 = 3$	0.0717	0.572
$\theta_0 = 4$	0.0471	0.762
$\theta_0 = 5$	0.0410	0.951

V. Experimental Verification

A. *Experiment I condition*

In this research, an experiment using an experimental vehicle, named FPEV-5, was conducted to evaluate the proposed method. The experimental setup and experimental condition are shown in Fig. 8 and Table. III. The transmitter and receiver coils designed in the conventional study [18] are used. The vehicle's speed was controlled to maintain 1 [m/s], and the driver steered the vehicle to keep it running straight. The AM was achieved by tilting the transmitter coil against the lane. θ_0 were shifted by 1 [deg] at a time from 0 to 5 [deg], and 20 runs were made for each value of the AM. The value of the LM was set to 50 [mm] when passing through the center

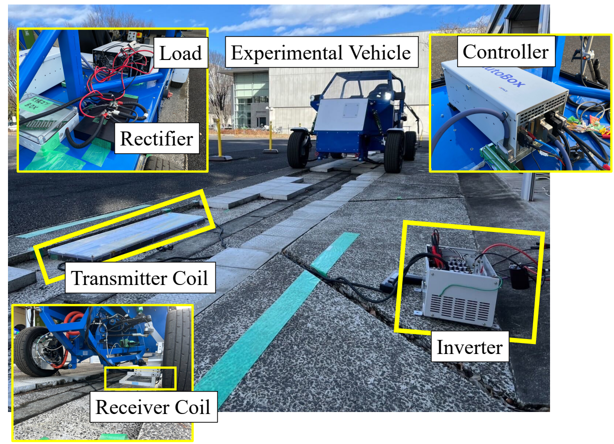

Fig. 8: Setup of experiment I.

TABLE III: Condition of experiment I.

Parameter	Value	Unit
v	1.00	m/s
f	83.3	kHz
$V_{1\mathrm{dc}}$, $V_{2\mathrm{dc}}$	25.0, 25.0	V
L_1, L_2	233, 92.6	μH
C_1, C_2	15.1, 38.9	nF
R_1, R_2	165, 158	mΩ
l_1	0.500	m
l_2	0.400	m

of the transmitter coil. Additionally, AM online estimation calculation was conducted by a controller shown in Fig. 8.

B. *Result of Experiment I*

First, current waveforms of one pattern each are shown in Fig. 9 as representative of 20 runs in each pattern. As the angle increases, the amount of change in LM increases, and the shape of the current waveform changes significantly. Second, the AM on-line estimation result is shown in Fig. 10. The mean and standard error values for each pattern are plotted with error bars. The estimated AM is slightly smaller than the true value, but the value is within one degree of error. In low AM conditions like 0, 1, and 2 [deg], the change in the current waveforms at each angle is clear. However, in high AM conditions like 3, 4, and 5 [deg], as can be seen in Fig. 9, the larger the angle becomes, the smaller the change in the current waveforms at each angle becomes. In the early phase of the power transfer, the coupling is low in the area, making it difficult to see a significant difference. However, as the estimation error is below 1 [deg] in all conditions, it can be said that the proposed AM estimation method is effective in steering control.

C. *Experiment II condition*

In this section, an experimental validation with vehicle steering control is shown. The experimental setup and experimental condition are shown in Fig. 11 and Table. IV. A white line was drawn in the center of the DWPT lane, and a camera was mounted on the back of the vehicle to visually provide

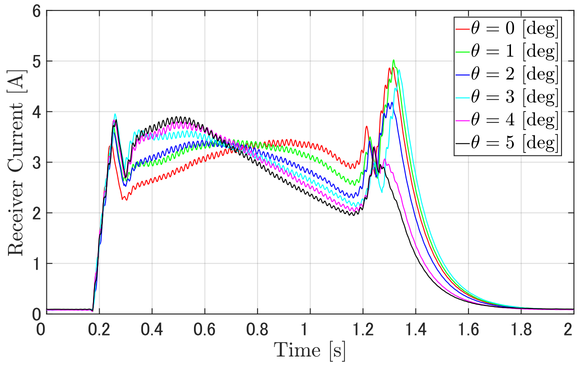

Fig. 9: Current waveforms.

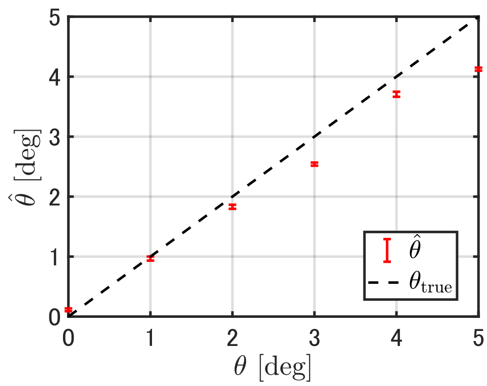

Fig. 10: Angular misalignment estimation result.

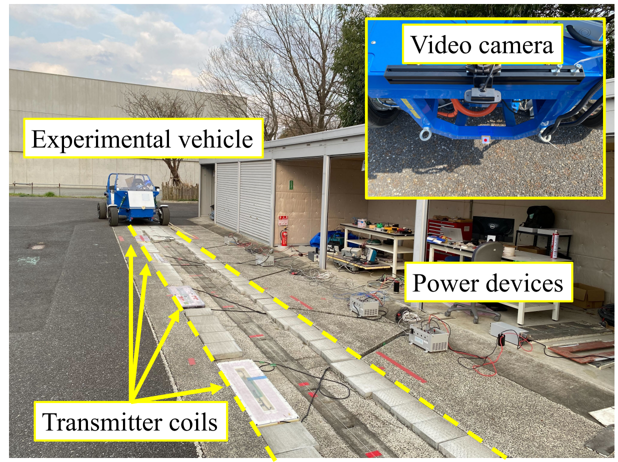

Fig. 11: Setup of experiment II.

TABLE IV: Parameters of experiment II.

Parameter	Value	Unit
v	1.00	km/h
f	85.0	kHz
$V_{1\text{dc}}$, $V_{2\text{dc}}$	35.0, 35.0	V
l_1	0.500	m
l_2	0.200	m
$Q_{Y_{\text{cg}}}$	1.00×10^{-6}	-
Q_θ	1.00×10^{-2}	-
$R_{Y_{\text{cg}}}$	1.00×10^{-3}	-
τ_β	5.00×10^{-2}	s
K_β	3.00×10^{-1}	-

the vehicle's LM. In experiment II, the vehicle's speed was controlled to maintain 1 [km/h]. The initial AM, θ_0, was varied from 1, 3, and 5 [deg]. The experiment was conducted using the proposed method with an initial estimated value of AM, $\hat{\theta}_0$, and the conventional method. The vehicle's active steering control was achieved by the electric power steering (EPS). The EPS is driven by a DC motor that performs position control by giving a steering angle command.

D. Result of Experiment II

Experimental results are shown in Fig. 12. In all figures, the section where the EV is passing above the transmitter coils is colored yellow. The steering control system properly activates to keep the lane without going out of the DWPT lane and gets electric power even on the second and subsequent coils, as shown in Fig. 11(a) and (b). This is mainly because θ_0 estimation is accurate, as shown in Fig. 11(c), and this θ information was also taken into account in the estimation of LM. Here, the true value of θ is obtained by adding the integral of the θ_0 and the yaw rate obtained from an IMU. However, it was confirmed that without $\hat{\theta}_0$ estimation, as in the conventional method, an appropriate estimation of the LM could not be conducted, resulting in a course out or large LM. This causes the vehicle to have too much LM to receive power. In Fig. 11(d), the true value of LM seen from the back of the vehicle, Y_{video}, calculated by image processing, is shown. From this figure, it can be seen that the convergence of LM is higher with the proposed method than with the conventional method. Figure 11(e) shows a comparison of the RMSE of LM for 0 [mm] when this experiment was performed four times, each with different $\hat{\theta}_0$. Error bars in the graph indicate the respective standard errors. The proposed method succeeds in lane-keeping in all patterns, and the LM is within the range of the power transfer, but with the conventional method, the LM increases as $\hat{\theta}_0$ increases. Moreover, in the case of $\hat{\theta}_0 = 5$ [deg], it was completely off the DWPT lane, and an accurate LM value could not be obtained.

VI. Conclusion

In this paper, a new method for estimating AM based on DC current on the receiver side in DWPT systems was proposed, utilizing the geometric relationship derived from LM values obtained from the current-map. From the simulation and experimental results, the proposed method was found to be able to estimate AM, resulting in enhancing LM estimation and control performance. In future work, we aim to improve the practicality of EV motion control in DWPT by combining LM control and longitudinal stopping control.

Acknowledgment

This work was partly supported by JST-Mirai Program Grant Number JPMJMI21E2, Japan.

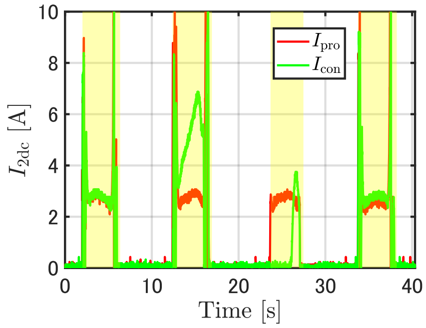

(a) Receiving side current ($\theta_0 = 1$ [deg]).

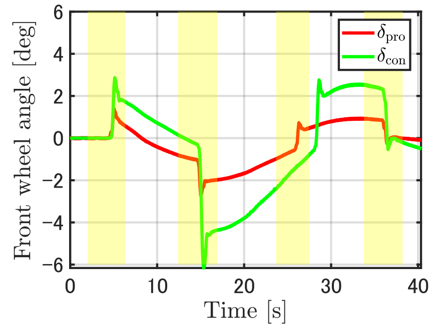

(b) Steering angle ($\theta_0 = 1$ [deg]).

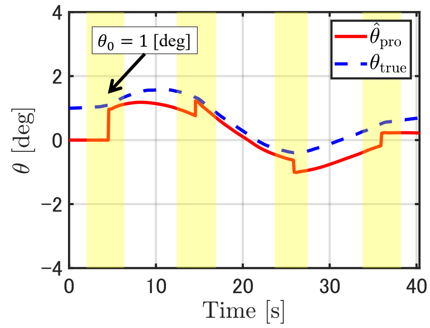

(c) Estimated AM ($\theta_0 = 1$ [deg], Proposed method only).

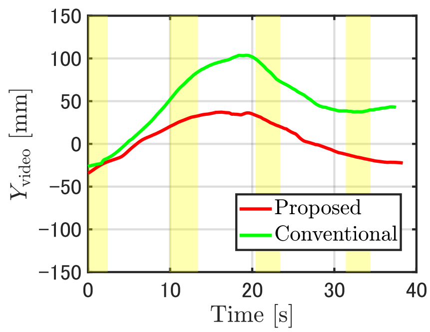

(d) LM ($\theta_0 = 1$ [deg]).

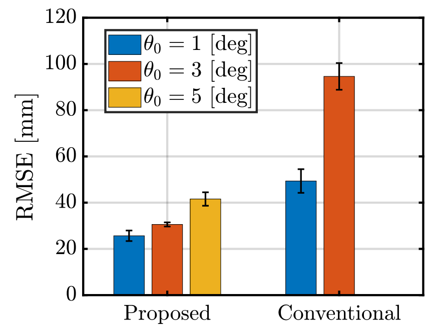

(e) RMSE comparison of LM.

Fig. 12: Results of experiment II.

References

[1] S. Yui and K. Furuya, "V2X Products and Social Implementation in Japan-Prospects from a "Global Warming Problem" Perspective," in *IEEJ Journal of Industry Applications*, vol. 12, no. 3, pp. 541-547, 2023.

[2] G. A. Covic and J. T. Boys, "Inductive Power Transfer," in *Proceedings of the IEEE*, vol. 101, no. 6, pp. 1276-1289, June 2013.

[3] N. Shinohara, "Power without wires," in *IEEE Microwave Magazine*, vol. 12, no. 7, pp. S64-S73, Dec. 2011.

[4] D. Gunji, O. Shimizu, S. Nagai, T. Fujita, and H. Fujimoto, "Greenhouse Gas Emission Evaluation Including Infrastructure for Passenger Electric Vehicles with Dynamic Wireless Power Transfer," in *IEEJ Journal of Industry Applications*, March 2025.

[5] A. Ahmad, M. S. Alam, Y. Rafat, and S. Shariff, "Designing and demonstration of misalignment reduction for wireless charging of autonomous electric vehicle," *eTransportation*, vol. 4, May 2020.

[6] J. Thalapil Vaheeda and B. George, "TMR Sensor-Based Detection of EVs in Semi-Dynamic Traffic for Optimal Charging," in *IEEE Transactions on Intelligent Transportation Systems*, vol. 23, no. 8, pp. 13721-13730, Aug. 2022.

[7] R. Tavakoli, T. Shabanian, E. M. Dede, C. Chou and Z. Pantic, "EV Misalignment Estimation in DWPT Systems Utilizing the Roadside Charging Pads," in *IEEE Transactions on Transportation Electrification*, vol. 8, no. 1, pp. 752-766, March 2022.

[8] Y. Tian, Z. Zhu, L. Xiang and J. Tian, "Vision-Based Rapid Power Control for a Dynamic Wireless Power Transfer System of Electric Vehicles," in *IEEE Access*, vol. 8, pp. 78764-78778, 2020.

[9] V. Cirimele et al., "The Fabric ICT Platform for Managing Wireless Dynamic Charging Road Lanes," in *IEEE Transactions on Vehicular Technology*, vol. 69, no. 3, pp. 2501-2512, March 2020.

[10] I. Cortes and W. -j. Kim, "Lateral Position Error Reduction Using Misalignment-Sensing Coils in Inductive Power Transfer Systems," in *IEEE/ASME Transactions on Mechatronics*, vol. 23, no. 2, pp. 875-882, April 2018.

[11] A. Babu and B. George, "Sensor System to Aid the Vehicle Alignment for Inductive EV Chargers," in *IEEE Transactions on Industrial Electronics*, vol. 66, no. 9, pp. 7338-7346, Sept. 2019.

[12] Y. Louca, E. A. ElGhanam, M. S. Hassan and A. H. Osman, "Design and Modeling of Auxiliary Misalignment Detection Coils for Dynamic Wireless Electric Vehicle Charging Systems," *2021 IEEE Transportation Electrification Conference and Expo (ITEC)*, Chicago, IL, USA, 2021, pp. 125-129,

[13] J. Wang, L. Wan, C. Cai, M. Xue, Y. Du, and J. Zhang, "A Dual-Side Magnetic Integration – Based Receiver Detection Method of Long-Track DWPT System," in *IEEE Transactions on Power Electronics*, vol. 39, no. 6, pp. 7752-7765, June 2024.

[14] H. Sun, X. Ma, R. Q. Hu, and R. Christensen, "Precise Coil Alignment for Dynamic Wireless Charging of Electric Vehicles with RFID Sensing," in *IEEE Wireless Communications*, vol. 32, no. 1, pp. 182-189, February 2025

[15] R. Tavakoli and Z. Pantic, "ANN-based algorithm for estimation and compensation of lateral misalignment in dynamic wireless power transfer systems for EV charging," *2017 IEEE Energy Conversion Congress and Exposition (ECCE)*, Cincinnati, OH, USA, 2017, pp. 2602-2609

[16] A. N. Azad, A. Echols, V. A. Kulyukin, R. Zane and Z. Pantic, "Analysis, Optimization, and Demonstration of a Vehicular Detection System Intended for Dynamic Wireless Charging Applications," in *IEEE Transactions on Transportation Electrification*, vol. 5, no. 1, pp. 147-161, March 2019.

[17] T. Koishi, B. -M. Nguyen, O. Shimizu and H. Fujimoto, "Receiving Side Current-Based Lateral Misalignment Estimation and Automated Steering Control for Dynamic Wireless Power Transfer," in *IEEE Journal of Emerging and Selected Topics in Industrial Electronics*, vol. 6, no. 1, pp. 41-52, Jan. 2025

[18] O. Shimizu, T. Fujita, S. Nagai, H. Fujimoto, and Y. Omori, "Development of Dynamic Wireless Power Transfer Coils for 3rd Generation Wireless In-Wheel Motor," in *IEEJ Transactions on Industry Applications*, vol. 141, no. 8, pp. 638 – 645, 2021.